pH-Responsive Poly(acrylic acid) Core Cross-Linked Star Polymers: Morphology Transitions in Solution and Multilayer Thin Films

Luke A. Connal,[†] Qi Li,[‡] John F. Quinn,[‡] Elvira Tjipto,[‡] Frank Caruso,*[,‡] and Greg G. Qiao*[,†]

Polymer Science Group and the Centre for Nanoscience and Nanotechnology, Department of Chemical and Biomolecular Engineering, The University of Melbourne, Parkville, Victoria 3010, Australia

Received August 30, 2007; Revised Manuscript Received January 23, 2008

ABSTRACT: Star polymers show great promise for a range of applications, including drug delivery and advanced coatings. Their unique solution properties and high functionality also make them attractive building blocks for the preparation of nanostructured thin films. This article describes the preparation of a poly(acrylic acid) (PAA)-based core cross-linked star (CCS) polymer by the "arm first" approach and its assembly into multilayered films by the layer-by-layer (LbL) method. Synthesis of the PAA star polyelectrolyte was achieved by preparing an acid protected polymer, poly(*tert*-butyl acrylate), by atom transfer radical polymerization and reacting it with a divinyl monomer (divinylbenzene), followed by deprotection. The PAA star polyelectrolyte displayed pH-responsive behavior in solution, as studied by dynamic light scattering, where a reversible size change was observed in response to pH changes. At pH 8–10, the acrylic acid segments are fully charged, adopting a more stretched conformation, and larger diameters (∼30 nm) were observed. When the pH decreases, and associated protonation of the acid segments occurs, the PAA chains adopt a more coiled conformation, and the diameters decrease to ∼23 nm at pH 2. The PAA star polymer was LbL assembled with poly(allylamine hydrochloride) (PAH) at different pH conditions to form pH-responsive multilayer films. The PAA star polymer/PAH multilayer films showed distinct morphology changes in response to post-treatment with different pH solutions. At pH 11, the star polymer adopted a stretched conformation and smoother films were obtained, whereas at pH 2, grain domains were visible and comparatively rougher films were formed.

Introduction

In recent times, hyperbranched polymers, a relatively new class of macromolecules, have received significant attention from both academia and industry.[1] Because of their unique physical properties and functionality, they have found applications in a variety of areas, including encapsulation, sensing, catalysis, electronics, optics, and biological engineering.[1] The significance of hyperbranched polymers is not only due to their unique properties in solutions, e.g., viscosity and solubility, but also because of their functionality, both in solution or in thin films. Layer-by-layer (LbL) assembly, which is typically based on the alternate adsorption of oppositely charged polyelectrolytes, has become a convenient and versatile technique for the preparation of ultrathin films with controlled nanostructure and functionality.[2] Materials as diverse as polymers,[2b] inorganic nanoparticles,[3] and biological macromolecules[4] have been assembled into multilayer thin films. Dendrimers, due to their unusual hyperbranched structure and unique functionality, can be included into multilayer thin films for applications such as sensing and controlled release.[5] Amine-[6] or acid-capped[7] dendrimers have been used to prepare thin films by electrostatic or hydrogen-bonding interactions. These dendrimer species are pH-responsive and are of interest in applications such as drug uptake and release as the dendrimer nanoenvironment can be well controlled.[8] Some other methods to incorporate dendrimers in multilayer films include the use of covalent bonding[9,10] or coordination chemistry.[11] Although the use of dendrimers in such films is promising, their synthesis involves multiple steps and can be complex and costly.

A viable alternative to dendrimers is the use of star polymers. The salient properties of dendrimer materials, such as polyvalency and a controlled nanoenvironment, can be realized by these star structures, while minimizing cost. The advent of living polymerization techniques has enabled researches to synthesize well-defined molecular architectures, including star polymers. Two general strategies for preparing star polymers have emerged: the "core first" technique, where a multifunctional initiator is used to initiate polymerization,[12] and the "arm first" approach, where a living linear polymer (arm) is coupled with a difunctional monomer to yield core cross-linked star (CCS) polymers. CCS polymers are unique three-dimensional structures that consist of a cross-linked core with a high number of arms radiating from this core. Recent efforts have demonstrated that these macromolecules can be effectively synthesized by living radical polymerization techniques, including nitroxide mediated radical polymerization (NMRP),[13] reversible addition fragmentation chain transfer polymerization (RAFT),[14] and atom transfer radical polymerization (ATRP).[15] Degradable CCS polymers have also been synthesized by ring-opening polymerization.[16] Star polyelectrolytes are also interesting building blocks for assembly into multilayer thin films because they have a high charge density and can be readily modified to introduce various other functionalities. Further, they can be made with pH-responsive moieties, thereby conferring pH responsiveness to the resulting multilayer films.

Herein, linear poly(*tert*-butyl acrylate) (an acid-protected polymer) is synthesized via ATRP. This macroinitiator is then used to form a star polymer utilizing the "arm first" technique; this synthesis was optimized for maximum star yield. Deprotection of the pendant *tert*-butyl group yields a poly(acrylic acid) (PAA) star polymer with high functionality. The star polyelectrolyte shows reversible pH-responsive behavior in solution, as studied by dynamic light scattering (DLS). We also report, to the best of our knowledge, the first example of utilizing star

* Corresponding authors. E-mail: gregghq@unimelb.edu.au; fcaruso@unimelb.edu.au.
[†] Polymer Science Group.
[‡] Center for Nanoscience and Nanotechnology.

10.1021/ma7019557 CCC: $40.75
Published on Web 03/13/2008

polymers to prepare multilayered thin films via the LbL methodology. Thin films were prepared by the alternate adsorption of the star polyelectrolyte and poly(allyamine hydrochloride) (PAH). These films were subsequently treated with solutions of different pH, resulting in drastic morphology changes in the films, as studied by atomic force microscopy (AFM). The star PAA/PAH films were also compared to the films assembled from linear PAA and PAH. Different film growth behaviors showing thicker films and unique film morphologies were observed, showing that the use of star polymers in thin films affords new materials with different physical properties. These results can be contrasted with those of other branched polymers, such as dendrimers. Dendrimers are considerably smaller in molecular size compared to CCS polymers; dendrimers previously reported in LbL films only have a M_w of around 15 kDa,[6,8] and the CCS polymers used in the current study have a M_w of 270 kDa, which makes this system quite unique. The use of the star polymers also adds greater versatility due to low number of synthetic steps in their preparation and easy functionalization.

Experimental Section

Materials. *tert*-Butyl acrylate (*t*BA; 98%), divinylbenzene (DVB; 80%), and *N,N,N′,N″,N″*-pentamethyldiethylenetriamine (PMDETA; 99%) were washed three times with 5% sodium hydroxide (NaOH), once with distilled water, and then distilled over calcium hydride. Copper(I) bromide (CuBr; 98%), methyl 2-bromopropionate (2MBP; 98%), trifluoroacetic acid (TFA; 99+%), poly(allylamine hydrochloride) (PAH, M_w = 70 000 g mol^{-1}) and poly(ethylenimine) (PEI, M_w = 25 000 g mol^{-1}) were used as received. All chemicals were purchased from Aldrich. Quartz crystal microbalance (QCM) electrodes (resonant frequency = 9 MHz, AT-cut) were purchased from Kyushu Dentsu (Nagasaki, Japan) and silicon wafers from MMRC Pty. Ltd., Australia. QCM electrodes were cleaned by treatment with a sulfuric acid/hydrogen peroxide (3:1) mixture (piranha solution). (*Caution!* piranha solution is highly corrosive. Extreme care should be taken when handling Piranha solution, and only small quantities should be prepared.) The RCA protocol (sonication in a 1:1 mixture of water and 2-propanol for 15 min, followed by heating at 70 °C for 10 min in a 5:1:1 mixture of water, H_2O_2 (30% in water), and a 29 vol % ammonia solution), was applied to clean the silicon wafers and hydrophilize the wafer surfaces. A Millipore RiOs/MilliQ system was used to produce high-purity water (Milli-Q) with a resistivity greater than 18 MΩ·cm.

Measurements. Gel permeation chromatography (GPC) was performed on a Shimadzu system with a Wyatt DAWN DSP multiangle laser light scattering detector (690 nm, 30 mW) and a Wyatt OPTILAB EOS interferometric refractometer (690 nm). THF was used as the eluent with three Phenomenex phenogel columns (500, 10^4, and 10^6 Å porosity; 5 μm bead size) operated at 1 mL min^{-1} with the column temperature set at 30 °C. Astra software (Wyatt Technology Corp.) was used to process the data using known d*n*/d*c* values to determine the molecular weight or an assumption of 100% mass recovery of the polymer where the d*n*/d*c* value was unknown. Monomer conversion was determined by gas chromatography using a Shimadzu GC 17-A gas chromatograph equipped with a DB-5 capillary column (30 m, 5% phenylsiloxane) and coupled to a GCMS-QP5000 mass spectrometer (injection temperature: 250 °C; initial column temperature: 40 °C; final column temperature: 250 °C heated at 10 °C min^{-1}). Monomer conversions were calculated from standard response vs concentration curves generated using pure monomers. Potentiometric titrations were conducted using a TPS WP81 pH−conductivity−salinity meter. Aqueous solutions of polymer were prepared (1 mg mL^{-1}) and titrated with 0.1 M NaOH. The pH values were plotted as a function of activity coefficient or the ionization degree, $\alpha = C_b/C_{AA}$, where C_b is the concentration of NaOH added to the solution and C_{AA} is the concentration of acrylic acid in solution. Dynamic light scattering (DLS) was performed using a Malvern 4700 unit with a 10 mW Ar ion laser operated at 488 nm. Analysis was performed at an angle of 90° and a constant temperature of 25 °C. Samples were made up at 1 mg mL^{-1} in 0.01 M NaOH and diluted dropwise with 0.1 M NaOH or 0.1 M HCl to adjust the pH. Transmission electron microscopy (TEM) measurements were conducted on a Philips CM120 BioTWIN instrument, operating at 120 kV. Positive staining of PAA segments was achieved by mixing an equal amount of basic (pH 8) PAA star (0.0001 mg mL^{-1}) solution with a lead acetate saturated solution for 2 h. A drop (1 μL) of this solution was cast onto a Formvar-coated gold TEM grid, the drop was not allowed to dry, and the grid was subsequently washed with water multiple times. A home-built QCM device with a frequency counter was used to determine the deposited mass after each adsorption step according to the Sauerbrey equation.[17] The resonant frequency of the gold-coated electrodes was ca. 9 MHz. The connections of the QCM electrode were sealed and protected with silicone rubber to prevent degradation during immersion in the solutions. Atomic force microscopy (AFM) images of air-dried multilayer films on silicon wafers were captured by using an Asylum MFP-3D AFM operating in AC mode. The scan areas were 5 μm × 5 μm or 1 μm × 1 μm. Silicon tips with a radius of <10 nm, spring constant of ~40 N m^{-1}, and resonance frequency of ~300 kHz were used.

General Procedure for the Synthesis of the Poly(*tert*-butyl acrylate) Macroinitiator. A mixture of *t*BA (15 mL, 113.6 mmol), CuBr (0.2716 g, 1.8 mmol), PMDETA (396 μL, 1.8 mmol), and 2-MBP (211 μL, 1.8 mmol) was added to a Schlenk flask and degassed by three freeze–pump–thaw cycles. The flask was then immersed in an oil bath at 60 °C and heated for 1 h. A sample of the reaction mixture was taken for GC analysis. The reaction mixture was diluted with THF (100 mL), passed through a column of basic alumina and celite (4:1), concentrated, and precipitated into 50% methanol/water (2 L) at −18 °C. The precipitate was collected by vacuum filtration, and the precipitation repeated to afford the P*t*BA macroinitiator (**1**) as a white solid (70% yield, M_n = 10 500 g mol^{-1} [GPC]; M_n = 9500 g mol^{-1} [NMR]; PDI = 1.13; D_H = 3.5 nm).

General Procedure for the Synthesis of Poly(*tert*-butyl acrylate)-Based CCS. A mixture of P*t*BA macroinitiator (**1**) (M_n = 10 500 g mol^{-1}, 2 g, 0.2 mmol), DVB (252 μL, 1.8 mmol), CuBr (29 mg, 0.2 mmol), and PMDETA (125 μL, 0.6 mmol) in *p*-xylene (13 mL) was added to a Schlenk flask and degassed by three freeze–pump–thaw cycles. After 40 h, a sample was taken from the reaction mixture and analyzed directly by GC. The mixture was diluted with THF (100 mL), passed through a column of basic alumina and celite (4:1), concentrated and precipitated into 50% methanol/water (1 L) at −18 °C, and collected by filtration to afford a colorless solid (**9**), which was analyzed by GPC-MALLS (yield = 85%, M_n = 397 000 g mol^{-1} [GPC], PDI = 1.2).

General Procedure for the Conversion of Poly(*tert*-butyl acrylate) CCS to Poly(acrylic acid) CCS. A round-bottom flask (100 mL) was charged with star P*t*BA (**6**) (M_n = 397 000; 1.5 g; ~9.3 mmol of *tert*-butyl ester) followed by dichloromethane (40 mL). The mixture was allowed to stir for 15 min to dissolve the polymer. Excess trifluoroacetic acid (TFA; 4.4 mL, 58.3 mmol) was added. The mixture was allowed to stir at room temperature for 24 h; samples were constantly taken for NMR analysis. After 24 h a yellow precipitate had formed, and dichloromethane and TFA were removed by rotary evaporation. The polymer was washed three times with acetone, then dissolved in methanol, precipitated into chloroform, and collected by filtration to afford a colorless solid (**8**), which was analyzed by GPC-MALLS. The star mixture was then fractionally precipitated by dissolving the star polymer (**8**, 1.0 g) into methanol (50 mL) and adding chloroform (40 mL). The high molecular weight precipitate (pure star polymer) was filtered and dried (yield = 40%, M_n = 270 200 g mol^{-1} [GPC], PDI = 1.09).

Preparation of Star PAA/PAH Multilayer Films. The substrate (QCM electrode or silicon wafer) was initially exposed to an aqueous solution of PEI (0.5 mg mL^{-1}, 0.1 M NaCl) for 15 min and then rinsed by three sequential dips into Milli-Q water, followed by drying with a gentle stream of nitrogen. The substrate was then dipped into a PAA-based star polymer (**8**) solution (0.5 mg mL^{-1},

Scheme 1. Synthesis of Poly(acrylic acid) (PAA)-based Core Crosslinked Star (CCS) Polymer via the "Arm First" Approach[a]

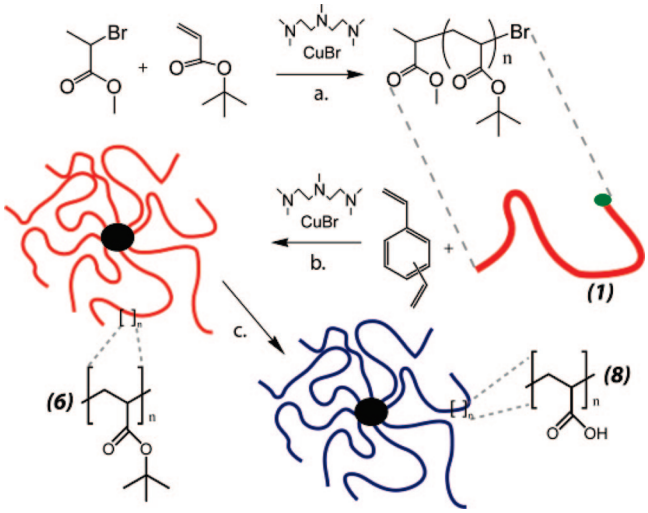

[a] Conditions: (a) 60 °C, bulk, 1 h; (b) 100 °C, anisole, 40 h; (c) trifluoroacetic acid, chloroform, 24 h.

0.1 M NaCl, pH 3.5 or pH 7.5) for 15 min, followed by the rinsing and drying protocol described above. Multilayer films were then assembled by continuing this sequential adsorption process, alternating between a cationic PAH solution (0.5 mg mL^{-1}, 0.1 M NaCl, pH 7.5) and the anionic star polymer (**8**) solution, until the desired layer number was reached. The solution pH was adjusted using HCl or NaOH and was measured with a Mettler-Toledo MP220 pH meter.

Results and Discussion

In a three-step process, linear poly(*tert*-butyl acrylate) was initially synthesized via ATRP; this macroinitiator was then coupled into the CCS star polymer by reaction with divinylbenzene. Finally, deprotection of the *tert*-butyl groups yields the star poly(acrylic acid), as shown in Scheme 1.

Synthesis of Linear Poly(*tert*-butyl acrylate). Copper-catalyzed ATRP polymerization of *t*BA initiated by methyl 2-bromopropionate in bulk at 60 °C (Scheme 1, step a) was used to prepare P*t*BA macroinitiator. For the formation of the CCS polymers it has previously been shown[15b] an arm molecular weight of ~10 000 g mol^{-1} is ideal for the coupling step. Linear P*t*BA of M_n = 10 500 g mol^{-1} as determined by GPC-MALLS, was synthesized with a polydispersity of 1.13 (**1**). Characterization via NMR showed the peaks from the methyl hydrogens of the *tert*-butyl ester at 1.43 ppm. The methyl ester of the end group showed a signal at 3.7 ppm. Calculation of the signal integration of this peak relative to the peak due to the *tert*-butyl ester gave a M_n = 9500 g mol^{-1}. This is in good agreement with the value from GPC-MALLS. This linear poly(*tert*-butyl acrylate) (**1**) was used to prepare the CCS polymers.

Synthesis of Poly(*tert*-butyl acrylate)-Based CCS. The arm first approach was utilized to prepare star polymers, whereby linear P*t*BA (**1**) was reacted under ATRP conditions to form CCS polymer structures (Scheme 1, step b). The coupling of the bromine functional P*t*BA with DVB under ATRP conditions showed good control. It has been reported that during the synthesis of these star structures (not specific to the controlled radical technique employed) there will be residual linear polymer in the mixture.[13,15] Therefore, it is important to optimize the reaction conditions to maximize the yield of the star polymer. There are two main conditions that were found to significantly affect the star formation: the ratio of cross-linker (DVB) to macroinitiator, r_0, and the original concentration of macroinitiator in the solution mixture, [P*t*BA]$_0$. The shape of the GPC chromatogram was used to evaluate the star structure. The evolution of higher molecular weight species (at low elution volumes) is evidence of star formation.

Initially, [P*t*BA]$_0$ was varied from 5 to 15 mM, while maintaining r_0 = 14 (Table 1 and Figure 1a). When [P*t*BA]$_0$ was increased from 5 to 15 mM, a large increase in the number of arms, molecular weight, and yield of the star were all noted; above 15 mM the reaction mixture gelled. The ratio of cross-linker to P*t*BA (r_0) was then varied from 6 to 14, while maintaining [P*t*BA]$_0$ = 15 mM (Table 1 and Figure 1b). All reactions showed high yield of star polymer, and an increase in the number of arms with increasing amount of cross-linker was observed. In general, the higher the initial macroinitiator concentration, the higher the percentage of star species formed, and increasing the amount of cross-linker increased the molecular weight of the star. We found r_0 = 9 and [P*t*BA]$_0$ = 15 mM to be the optimal conditions for the P*t*BA star system. Typically, the size of the DVB cores is around 10 nm.[16] The star polymer (**6**), with M_w = 397 000 g mol^{-1} in 85% yield and ~32 arms, was then used in the deprotection step to yield the acid star polymer.

Cleavage of the *tert*-Butyl Ester. The deprotection of the *tert*-butyl group was achieved by treatment of the P*t*BA star polymer with an excess of trifluoroacetic acid in dichloromethane (Scheme 1, step c). Within 24 h a brown precipitate formed. This polymer showed a marked difference in solubility compared to the P*t*BA CCS polymer. The formed product was washed with acetone and reprecipitated from methanol into chloroform. This star polymer (**8**) was soluble in aqueous and polar organic solvents. The cleavage of the butyl group was confirmed by ^{1}H NMR spectroscopy, as shown in Figure 2 (note the disappearance of the peak at 1.43 due to the *t*BA groups). To quantify the acrylic acid content, an acid–base titration was performed, proving more than 90% of the *tert*-butyl groups were cleaved.

GPC was performed on this polymer with methanol as the mobile phase to examine whether the star polymer structure remained intact. Figure 3 (top trace) shows that the deprotection procedure did not affect the architecture of the star PAA. The molecular weight decreased to 270 200 g mol^{-1}, which corresponds to a decrease of 30% of the original star polymer. This is reasonable as the *tert*-butyl group removed from the polymer arms was a large proportion of the repeat unit. The theoretical value for 100% cleavage would result in a new molecular weight of 252 000 g mol^{-1}, which agrees well with the experimental value. Fractional precipitation with methanol/chloroform was performed, and the pure star was isolated (Figure 3, bottom trace). This pure star was used to analyze the pH-dependent behavior of the star polymer.

Solution Properties of PAA-Based CCS. The activity coefficient (α) and hence the degree of ionization of the CCS PAA were calculated by pH-titration experiments. Figure 4 shows the behavior of the star PAA compared to linear PAA synthesized via ATRP (after deprotection of P*t*BA) and linear PAA purchased from Aldrich. The star PAA has a slightly higher p$K_{a,app}$ of 6.5 (approximated from α = 0.5), while both linear polymers have a p$K_{a,app}$ = 5.8, which is similar to literature values.[18] This disparity is in agreement with predicted theory[19] and recent experimental results:[20] the higher osmotic pressure inside the star polymer causes a partial reversal of ionization, where there are less charged ions in the confined regions of the star poly(electrolyte)[20] and hence a higher pH requirement to reach α = 0.5. We note that linear PAA itself has a range of pK_a values in the literature[28] depending on the solution conditions. For the purpose of this work, we compared

Table 1. Summary of Core Cross-Linked Star (CCS) Synthesis[a]

	PtBA macroinitiator			CCS polymer				
polymer	M_n[b]	$[PtBA]_0$ (mM)[c]	r_0[d]	M_w(GPC)[b]	PDI[b]	no arms[e]	arm conv (%)[f]	D_H[g] (nm)
2	10 500	5	14	175 000	1.20	12	48	15
3	10 500	10	14	232 000	1.20	17	52	16
4	10 500	15	14	468 000	1.13	38	81	23
5	10 500	15	6	375 000	1.18	30	76	20
6	10 500	15	9	397 000	1.12	32	85	22
7 (**4**)	10 500	15	14	468 000	1.13	38	81	23
8	poly(acrylic acid)			270 200	1.09	32	85	27[h]

[a] Reaction conditions: $[PtBA]_0 = [CuBr]_0 = [N,N,N',N'',N''$-pentamethyldiethylenetriamine$]_0/2$ and divinylbenzene (DVB), anisole, 100 °C, 40 h. [b] Polydispersity (PDI), number-average molecular weight (M_n), and weight-average molecular weight (M_w) were measured by gel permeation chromatography equipped with multiangle laser light scattering (GPC-MALLS). [c] $[PtBA]_0$ = overall initial concentration of PtBA macroinitiator. [d] r_0 = initial molar ratio of DVB to poly *tert*-butyl acrylate macroinitiator (PtBA). [e] Number of arms calculated from the formula = $Wf_{arms}M_{w,star}/M_{w,arms}$. [f] Calculated from integration of GPC concentration detector (DRI). [g] Calculated for THF. [h] Calculated for aqueous conditions.

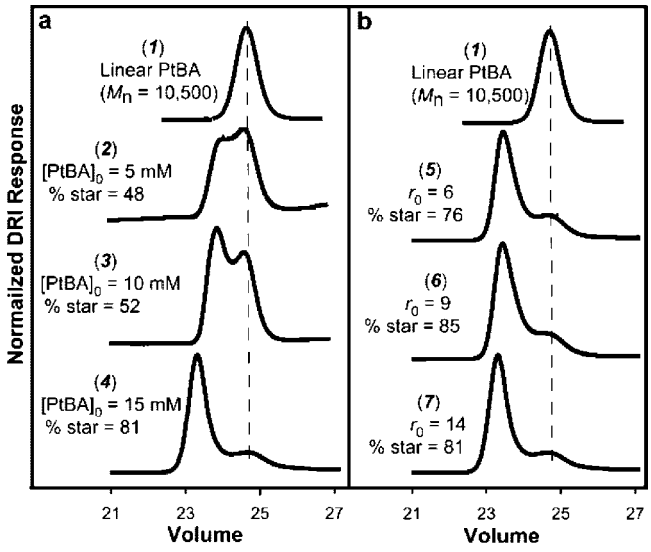

Figure 1. GPC chromatograms showing normalized concentration detector (differential refractive index) of star formation. (a) Concentration study, varying the initial concentration of macroinitiator, $[PtBA]_0$. (b) Stoichiometry study, varying the ratio of macroinitiator to cross-linker, r_0.

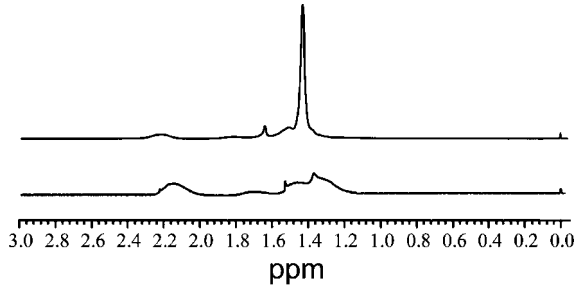

Figure 2. ^{1}H NMR spectroscopy showing the cleavage of *tert*-butyl groups of the star polymer to yield a PAA-based CCS polymer. Star poly(*tert*-butyl acrylate) (top) in deuterated chloroform and star PAA (bottom) in deuterated methanol.

star and linear analogues under the same solution conditions to emphasize their different solution behavior.

Dynamic light scattering was performed to analyze the hydrodynamic diameter of the PAA star at different degrees of ionization. An initial PAA star solution was made at pH 11, and then the pH was adjusted gradually to 2 and then back to alkaline conditions. All measurements were taken at an angle of 90° at 30 °C. Figure 5 shows the response of the PAA star to varying pH. At high pH, the acid segments of the star polymer are completely charged. Hence, the PAA arms are stretched and the star shows a maximum in hydrodynamic diameter (D_H) of

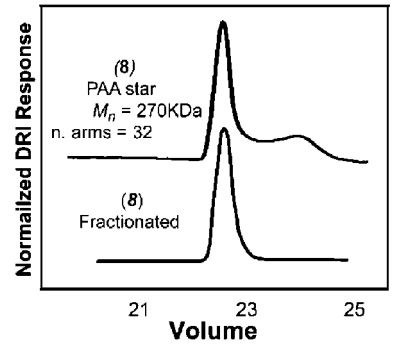

Figure 3. GPC chromatograms showing normalized concentration detector (differential refractive index) of star PAA mixture (top) and fractionated star PAA (bottom) in methanol.

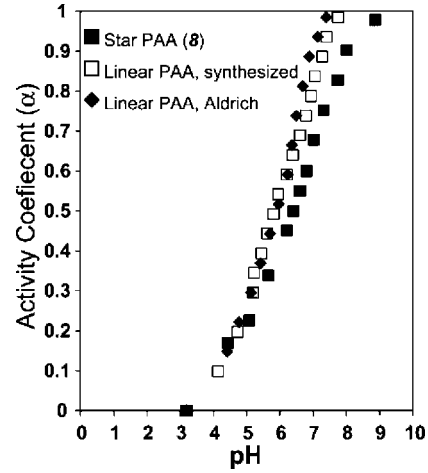

Figure 4. Activity coefficient (α) of star PAA (solid squares), linear PAA synthesized by ATRP (empty squares), and linear PAA from Aldrich (solid diamonds).

32 nm. When the degree of ionization decreases (i.e., pH decreases), the diameter decreases. Under these conditions, the PAA arms are in a coiled conformation and hence a smaller D_H (23 nm) is observed. When the pH was increased again, an increase in the diameters was observed, showing the conformational changes are largely reversible. In this case, the maximum D_H observed was 27 nm. This value is slightly lower than the initial size of the star polymer and can be explained by the increase in salt concentration of the solution as the pH is changed. This additional salt would cause screening of the charges on the star PAA, leading to a smaller size.

Multilayer Film Formation. The synthesis strategy outlined in this paper affords star polyelectrolytes with high functionality and unique solution properties, including pH-responsive behav-

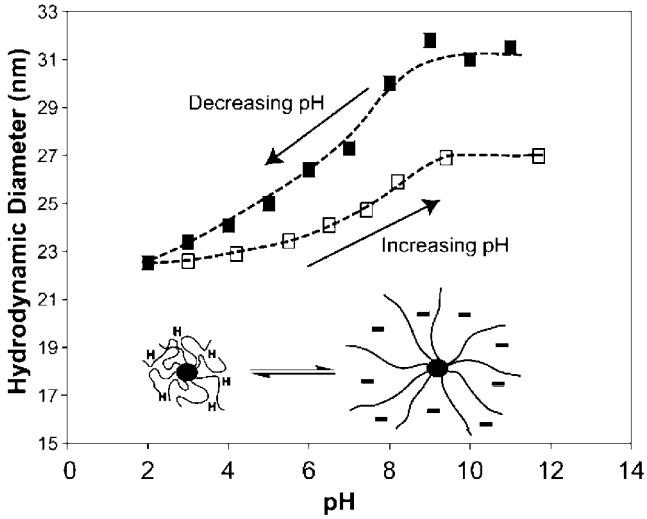

Figure 5. Hydrodynamic diameters (D_H) of star PAA (**8**) at varying pH and schematic representations of possible star configurations. Reducing pH from alkaline conditions (solid squares) and increasing pH from acidic conditions (open squares).

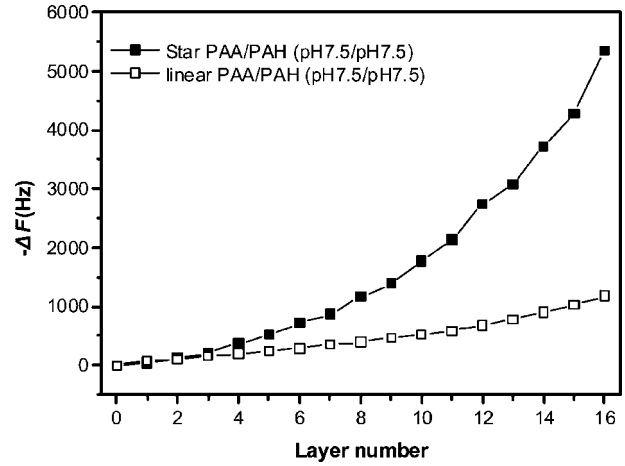

Figure 6. QCM frequency change as a function of layer number for star PAA/PAH multilayer films assembled from star PAA solutions at pH 7.5 and PAH at pH 7.5 (closed squares). As a control, the QCM frequency changes of linear PAA/PAH multilayers assembled from PAA at pH 7.5 and PAH at pH 7.5 (open squares) were also measured. All of the adsorption solutions have a polymer concentration of 0.5 mg mL^{-1} with 0.1 M NaCl added.

ior. These polymers can be used as building blocks to prepare a new class of functional multilayer films. These films may find applications in biosensing and drug delivery. For example, when a thin film of the pH-responsive star polymer is coated onto planar or colloidal supports, each CCS polymer can be designed to bind to a receptor for enzyme immobilization or as nanocontainers for drug loading and release. We chose to study the assembly of (star PAA/PAH) multilayer films and to investigate the response of these films to post-treatment with solutions of differing pH. This particular polymer combination was selected because of extensive earlier work on a similar system, PAA/PAH multilayers. It was reported that the thickness and surface morphology of (PAA/PAH) multilayer films are dramatically influenced by the pH of the individual polymer adsorption solutions.[21] Further, by controlling the pH, the bilayer thickness of a thin film can be tuned from 1 to 12 nm.

To investigate the assembly of multilayers using star PAA (**8**), films were assembled by the alternate adsorption of star PAA and PAH at pH 7.5. Sodium chloride (0.1 M) salt was added to each dipping solution. We have demonstrated above that the star polymer has a pK_a of ~6.5. Therefore, star polymer assembly at these pH values was expected to lead to regular film growth due to the charged nature of the star PAA under these conditions. Film buildup as a function of layer number was monitored with a QCM by following the frequency change, $-\Delta F$ (which is related to the mass adsorbed through the Sauerbrey equation[17]) (Figure 6). As a control, multilayer assembly from linear PAA and PAH at pH 7.5 (with 0.1 M salt added in each adsorption solution) was also investigated. The data show that the star PAA/PAH film growth (and hence the amount of material deposited) was significantly larger than the linear PAA/PAH system. The difference in growth is likely due to the different structure of the star polymer, arising from the highly cross-linked core (and therefore closely packed COOH or COO^- functional groups around the core) and its slightly higher pK_a value compared to the linear PAA (Figure 4). The film thickness of the (star PAA/PAH)$_8$ multilayer can be calculated from the total QCM frequency change of the multilayer, yielding a value of 91 nm.[22] This value is in good agreement with the thickness measured by AFM (80 nm).

The nonlinearity of the multilayer growth for the star PAA/PAH film may, in part, be due to interlayer chain diffusion.[23–25] Diffusion of polymer chains has been previously shown to cause exponential multilayer growth. However, it is unlikely that there is significant diffusion of the star PAA polymer because of its high molecular weight (~270 kDa) and globular structure. It is also possible that PAH could be the diffusing species in the multilayer films.

The star PAA/PAH multilayer films were further characterized by AFM to probe the pH-dependent surface morphology. In this case, films assembled with the star PAA adsorbed at pH 3.5 and PAH adsorbed at 7.5 were examined. This pH combination was selected as previous work by Rubner and coworkers has demonstrated that films assembled under these conditions are highly pH-responsive.[26] A 17-layer star PAA/PAH film assembled from pH 3.5/pH 7.5 with the star polymer as the outmost layer was first prepared on a PEI-coated silicon wafer (Figure 7a). AFM measurements indicate that this multilayer film has a thickness of 60 nm, and this value is similar to that obtained using ellipsometry (75 nm). The film exhibited a rough and porous surface, which arises due to the different salt concentrations between the dipping solutions (0.1 M salt) and Milli-Q water used during rinsing steps after each adsorption.[27] The star PAA/PAH multilayer film was further exposed to a pH 2 (Figure 7b) or a pH 11 (Figure 7c) aqueous solution for 1 min. By FTIR measurements (data not shown), at pH 2, the star PAA/PAH films showed a high proportion (~85%) of protonated carboxylic acid groups (−COOH). Conversely, at pH 11, the films showed a high proportion (~85%) of ionized carboxylic groups ($-COO^-$). PAH ionization determination by FTIR is complicated by overlapping peaks[28] and hence was not examined in this case. The pH 2-treated film (Figure 7b) showed a distinctly different surface morphology compared to the as-assembled film (Figure 7a). The "wormlike" surface is possibly due to phase separation within the film at low pH. The higher resolution image (Figure 7b inset) shows grain domains, which is attributed to the highly coiled conformation of the star PAA at low pH. The grain domains were not observed for pH 11-treated films (Figure 7c) because at this pH the PAA arms are largely charged and hence are likely to be extended on the surface. The morphology of the star PAA/PAH film when subjected to pH 11 treatment shows a minor change (Figure 7c,d), relative to the change observed after acidic post-treatment, suggesting that the change in the ionization of PAH is not a major driving force for the film rearrangement.

To further investigate the reversibility of the morphology transitions of the thin films in response to changes in pH, the

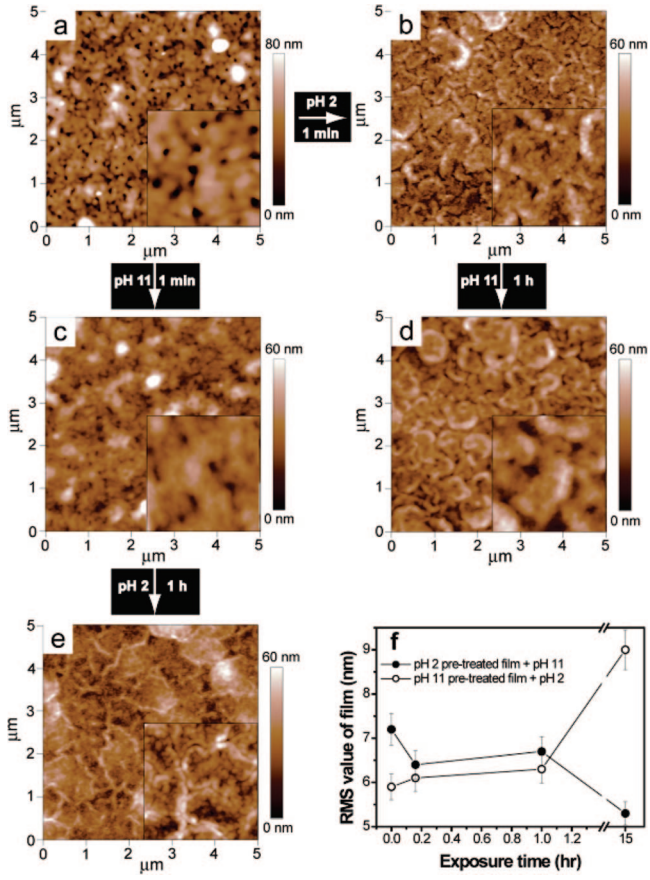

Figure 7. AFM images of PEI/(star PAA/PAH)$_8$/star PAA multilayer films assembled from a star PAA solution (pH 3.5, 0.1 M salt) and PAH (pH 7.5, 0.1 M salt) before (a) and after 1 min exposure to pH 2 (b) or pH 11 (c) solutions. The pH 2-treated film was further exposed to a pH 11 solution and the pH 11-treated films to a pH 2 solution for a different period of time. Images (d) and (e) represent the pH 2-treated film after 1 h exposure to a pH 11 solution and pH 11-treated film after 1 h exposure to a pH 2 solution, respectively. (f) Surface roughness (rms) of the films as a function of exposure time.

pH 2- and pH 11-treated films were further exposed to pH 11 and pH 2, respectively. The surface morphology as a function of exposure time was also investigated. The films were exposed to the solutions for 10 min, 1 h, and 15 h and then analyzed by AFM. Figure 7d represents the surface morphology of the pH 2-treated films after 1 h exposure to pH 11. The phase separation-induced "wormlike" surface was maintained while the grain domains visible in pH 2-treated films (Figure 7b) were not observed. With longer pH 11 exposure times, the surface of the pH 2-treated films largely maintained the surface morphology ("wormlike", no grain domains) but became smoother. The surface of the pH 11-treated film after exposure to pH 2 for 1 h (Figure 7e) was substantially different than pH 11-treated films (Figure 7c). The surface morphology of pH 11-treated films after pH 2 exposure was similar to films treated at pH 2 (Figure 7b) (i.e., a "wormlike" surface and grain domains). These similarities demonstrate the reversible pH behavior of the films. Figure 7f shows the rms values (related to surface roughness) of the pH-treated films as a function of the exposure time. The surface of pH 2-treated films became smoother with increasing exposure time to pH 11 solution, while the pH 11-treated films increased in roughness with increasing exposure to pH 2 solution. Figure 7f shows that the surface morphology of the film after the second pH treatment did not reach equilibrium after 1 h. Instead, more noticeable changes in surface morphology were observed for longer treatment times. This suggests that the polymers are quite constrained in the multilayer film and film rearrangement occurs quite slowly. The observations relating to these morphology changes are schematically illustrated in Figure 8.

Conclusions

ATRP has been used to polymerize an acrylic acid-protected monomer (*t*BA) to form P*t*BA, and this macroinitiator was coupled with divinylbenzene to synthesize a P*t*BA-based CCS polymer. Optimization of the star synthesis was obtained by varying the cross-linker stoichiometry and initial concentration of the macroinitiator in the reaction medium, with high concentrations giving the highest yield of star. Deprotection of the *tert*-butyl groups was easily achieved to afford a star polyelectrolyte. The reversible morphological response of the star polyelectrolytes with different pH were shown, both in solution and in thin films. In solution, a distinct size decrease in D_H was observed by DLS with decreasing pH, and an increase was noted when the pH was increased. At high pH, the PAA arms are fully charged; therefore, the arms are stretched and a higher D_H resulted. At low pH, the acid segments are protonated, and hence the PAA arms are in a coiled state, decreasing its

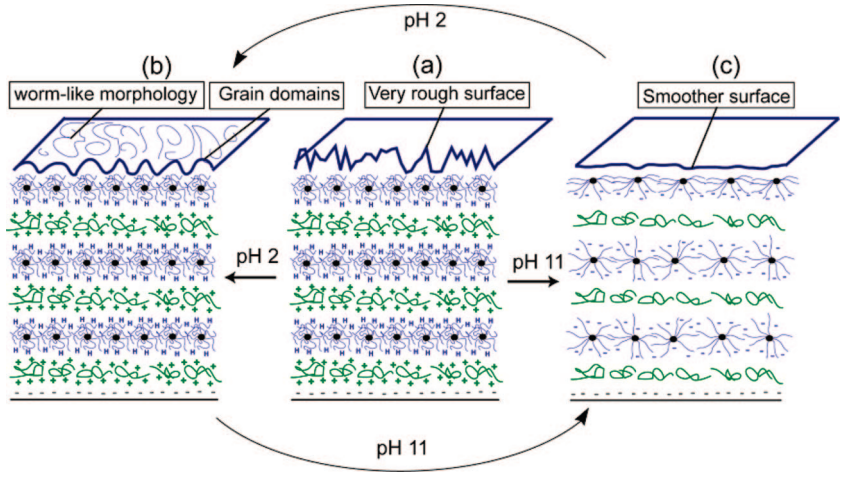

Figure 8. Schematic representation of morphology changes in hybrid star PAA/PAH multilayer films. (a) Before post-treatment−rough surface. (b) Film (a) treated with a pH 2 solution: protonation of the acrylic acid groups in star PAA induces a globular structure, showing grain boundaries (Figure 7b, inset) and a "wormlike" morphology (Figure 7b) which is possibly induced by phase separation of the star PAA at this pH. (c) Film (a) treated with a pH 11 solution: at this pH the star PAA is highly charged causing extension of the individual PAA arms, resulting in a relatively smooth surface (Figure 7c). This figure is not indicative of the actual ionization. Although significant interpenetration typically occurs in multilayer films, the polymers in this figure are shown as discrete layers for clarity.

size. These highly functional star polymers were shown to form stable films via LbL assembly. PAA star polymer films were successfully assembled when the star PAA was adsorbed at either pH 3.5 or pH 7.5 in alternation with PAH at pH 7.5. The star PAA/PAH (pH 3.5/pH 7.5) multilayer films showed distinct morphology changes in response to post-treatment with different pH solutions. In general, at high pH the star polymer assumes a stretched conformation and smoother films were formed, whereas at low pH, grain domains were visible and rougher films were formed. The results reported here demonstrate a "smart" star polyelectrolyte that shows pH-responsive changes in solution, and in thin films. This system can be compared with other branched structures, such as dendrimers, although the synthesis involved in core cross-linked star polymers is cheaper and more versatile. Work is currently underway to introduce coupling chemistries to prepare biologically addressable star PAA-based materials for use in solution and thin film applications.

Acknowledgment. This work was partially supported by an Australian Research Council under the Discovery Grant (F.C. and G.G.Q.) and Federation Fellowship (F.C.) schemes. Dr. Anthony Quinn is thanked for ellipsometry measurement, and James Wiltshire, Kuok Chiong Gan, and Tan Jing Fung are thanked for preliminary work in this area.

Supporting Information Available: Transmission electron micrograph of PAA star polymer. This material is available free of charge via the Internet at http://pubs.acs.org.

References and Notes

(1) (a) For reviews see: Voit, B. *J. Polym. Sci., Part A: Polym. Chem* **2000**, *38*, 505. (b) Hadjichristidis, N.; Pitsikalis, M.; Pispas, S.; Iatrou, H. *Chem. Rev.* **2001**, *101*, 3747. (c) Inoue, K. *Prog. Polym. Sci.* **2000**, *25*, 453. (d) Gao, C.; Yan, D. *Prog. Polym. Sci.* **2004**, *29*, 183.
(2) (a) Decher, G.; Hong, J.-D. *Ber. Bunsenges. Phys. Chem.* **1991**, *95*, 1430. (b) Decher, G. *Science* **1997**, *277*, 1232. (c) For a book see: Decher, G.; Schlenoff, J. B. *Multilayer Thin Films*; Wiley-VCH: New York , 2003.
(3) (a) Caruso, F.; Caruso, R. A.; Möhwald, H. *Science* **1998**, *282*, 1111. (b) Li, Q.; Quinn, J. F.; Wang, Y. J.; Caruso, F. *Chem. Mater.* **2006**, *18*, 5480.
(4) Lvov, Y.; Ariga, K.; Ichinose, I.; Kunitake, T. *J. Am. Chem. Soc.* **1995**, *117*, 6117.
(5) (a) Vossmeyer, T.; Guse, B.; Besnard, I.; Bauer, R. E.; Müllen, K.; Yasuda, A. *Adv. Mater.* **2002**, *14*, 238. (b) Khopade, A. J.; Caruso, F. *Biomacromolecules* **2002**, *3*, 1154.
(6) (a) Khopade, A. J.; Caruso, F. *Langmuir* **2002**, *18*, 7669. (b) Kim, B. Y.; Bruening, M. L. *Langmuir* **2003**, *19*, 94.
(7) Zhang, H.; Fu, Y.; Wang, D.; Wang, L.; Wang, Z.; Zhang, X. *Langmuir* **2003**, *19*, 8497.
(8) Khopade, A. J.; Caruso, F. *Nano. Lett.* **2002**, *2*, 415.
(9) Wang, J.; Jia, X.; Zhong, H.; Luo, Y.; Zhao, X.; Cao, W.; Li, M.; Wei, Y. *Chem. Mater.* **2002**, *14*, 2854.
(10) Vestberg, R.; Malkoch, M.; Kade, M.; Wu, P.; Fokin, V. V.; Sharpless, K. B.; Drockenmuller, E.; Hawker, C. J. *J. Polym. Sci., Part A: Polym. Chem.* **2007**, *45*, 2835–2846.
(11) Blasini, D. R.; Flores-Torres, S.; Smilgies, D. M.; Abruña, H. D. *Langmuir* **2006**, *22*, 2082.
(12) Robello, D. R.; Andre, A.; McCovick, T. A.; Kraus, A.; Mourey, T. H. *Macromolecules* **2002**, *35*, 9334.
(13) (a) Solomon, D. H.; Abrol, S.; Kambouris, P. A.; Looney, M. G. WO9831789, 1998, The University of Melbourne; A Process for preparing polymeric microgels. (b) Abrol, S.; Kambouris, P. A.; Looney, M. G.; Solomon, D. H. *Macromol. Rapid Commun.* **1997**, *18*, 755. (c) Pasquale, A. J.; Long, T. E. *J. Polym. Sci., Part A: Polym. Chem.* **2001**, *39*, 216. (d) Tsoukatos, T.; Pispas, S.; Hadjichristidis, N. *J. Polym. Sci., Part A: Polym. Chem.* **2000**, *39*, 320. (e) Bosman, A. W.; Vestberg, R.; Heumann, A.; Frechet, J. M. J.; Hawker, C. J. *J. Am. Chem. Soc.* **2003**, *125*, 715.
(14) (a) Lord, H. T.; Quinn, J. F.; Angus, S. D.; Whittaker, M. R.; Stenzel, M. H.; Davis, T. P. *J. Mater. Chem.* **2003**, *13*, 2819. (b) Moad, G.; Mayadunne, R. T. A.; Rizzardo, E.; Skidmore, M.; Thang, S. H. *Macromol. Symp.* **2003**, *192*, 1. (c) Zheng, G.; Pan, C. *Polymer* **2005**, *46*, 2802.
(15) (a) Solomon, D. H.; Qiao, G. G.; Abrol, S. S. WO 99/58588, 1999, The University of Melbourne, Process for Microgel Preparation. (b) Gurr, P. A.; Qiao, G. G.; Solomon, D. H.; Harton, S. E.; Spontak, R. J. *Macromolecules* **2003**, *36*, 5650. (c) Xia, J.; Zhang, X.; Matyjaszewski, K. *Macromolecules* **1999**, *32*, 4482. (d) Zhang, X.; Xia, J.; Matyjaszewski, K. *Macromolecules* **2000**, *33*, 2340. (e) Baek, K. Y.; Kamigaito, M.; Sawamoto, M. *Macromolecules* **2001**, *34*, 215; **2001**, *34*, 7629; **2002**, *35*, 1493. (f) Gao, H.; Matyjaszewski, K. *Macromolecules* **2007**, *40*, 399–401.
(16) (a) Wiltshire, J. T.; Qiao, G. G. *Macromolecules* **2006**, *39*, 4282. (b) Wiltshire, J. T.; Qiao, G. G. *Macromolecules* **2006**, *39*, 9018. (c) Biela, T.; Polanczyk, I. *J. Polym. Sci., Part A: Polym. Chem.* **2006**, *44*, 4214.
(17) Sauerbrey, G. *Z. Phys.* **1959**, *155*, 206.
(18) Sato, Y.; Hashidzume, A.; Morishima, Y. *Macromolecules* **2001**, *34*, 6121.
(19) Wolternil, J. K.; van Male, J. M.; Stuart, A. C.; Koopal, L. K.; Zhulina, E. B.; Borisov, O. V. *Macromolecules* **2002**, *35*, 9176.
(20) Plamper, F. A.; Becker, H.; Lanzendorfer, M.; Patel, M.; Whittemann, A.; Mallauff, M.; Muller, A. H. E. *Macromol. Chem. Phys.* **2005**, *206*, 1813.
(21) Shiratori, S. S.; Rubner, M. F. *Macromolecules* **2000**, *33*, 4213.
(22) Lvov, Y.; Ariga, K.; Ichinose, I.; Kunitake, T. *J. Am. Chem. Soc.* **1995**, *117*, 6117.
(23) Lavalle, P.; Gergely, C.; Cuisinier, F. J. G.; Decher, G.; Schaaf, P.; Voegel, J. C.; Picart, C. *Macromolecules* **2002**, *35*, 4458.
(24) Picart, C.; Mutterer, J.; Richert, L.; Luo, Y.; Prestwich, G. D.; Schaaf, P.; Voegel, J. C.; Lavalle, P. *Proc. Natl. Acad. Sci. U.S.A.* **2002**, *99*, 12531.
(25) Sun, B.; Jewell, C. M.; Fredin, N. J.; Lynn, D. M. *Langmuir* **2007**, *23*, 8452.
(26) Mendelsohn, J. D.; Barrett, C. J.; Chan, V. V.; Pal, A. J.; Mayes, A. M.; Rubner, M. F. *Langmuir* **2000**, *16*, 5017.
(27) Fery, A.; Scholer, B.; Cassagneau, T.; Caruso, F. *Langmuir* **2001**, *17*, 3779.
(28) Choi, J.; Rubner, M. F. *Macromolecules* **2005**, *38*, 116.

MA7019557